Hindawi Publishing Corporation
International Journal of Photoenergy
Volume 2013, Article ID 576952, 6 pages
http://dx.doi.org/10.1155/2013/576952

Research Article

Characterization and Modeling of CdS/CdTe Heterojunction Thin-Film Solar Cell for High Efficiency Performance

Hamid Fardi and Fatima Buny

Department of Electrical Engineering, University of Colorado Denver, Campus Box 110, P.O. Box 173364, Denver, CO 80217-3364, USA

Correspondence should be addressed to Hamid Fardi; hamid.fardi@ucdenver.edu

Received 6 May 2013; Revised 20 June 2013; Accepted 25 June 2013

Academic Editor: Gaetano Di Marco

Device simulation is used to investigate the current-voltage efficiency performance in CdTe/CdS photovoltaic solar cell. The role of several limiting factors such as back contact Schottky barrier and its relationship to the doping density and layer thickness is examined. The role of surface recombination velocity at back contact interface and extended CdTe layer is included. The base CdS/CdTe experimental device used in this study shows an efficiency of 16-17%. Simulation analysis is used to optimize the experimental base device under AM1.5 solar spectrum. Results obtained indicate that higher performance efficiency may be achieved by adding and optimizing an extended CdTe electron reflector layer at the back Schottky contact. In the optimization of the CdS/CdTe cell an extended electron reflector region with a barrier height of 0.1 eV and a doping density of 7×10^{18} cm^{-3} with an optimum thickness of 100 nm results in best cell efficiency performance of 19.83% compared with the experimental data.

1. Introduction

Among the thin-film solar cells, the commonly used are amorphous silicon, CuInGaSe2, and CdTe. At the present, the amorphous silicon solar cells have the largest market share in the world with less a fraction of one percent to CuInGaSe2 and about a few percen to CdTe cells. The benefit of using CdTe is for being a direct bandgap material with high absorption (in relationship with silicon) and the ease of device processing, can be deposited on glass in thin film typically a few micrometers and at low temperature [1–7].

Large-area CdTe photovoltaic panels can be economically fabricated, potentially making the CdTe thin-film solar cell a leading alternative energy source. However, the recorded experimental CdTe efficiency of 16.5% is much less than its theoretical maximum efficiency of 29%, where the open-circuit voltage of 0.845 V is well below what is expected for its bandgap of 1.42 eV [8–10]. The experimental measurement obtained by others is used as a benchmark for the optimization of the CdS/CdTe cell and for the development of the strategies to improve the efficiency referred to here as base device [11].

An important issue related to the limiting performance of the CdTe cells is the back contact. Experimental works show that the CdTe cells at back contact form Schottky barrier thus degrading the cell efficiency and performance [12–18]. Other limiting factors in performance of CdTe cells are related to the unavailability of the physical material properties which is at incubator status when compared with the mature technology of the silicon and silicon electronics [19–26].

The modeling approach adopted in this paper allows us to examine device design and the role of material parameters in the performance and efficiency of the cell. Device simulation is used to predict the characteristics of CdS/CdTe heterojunction solar cells by identifying material parameters essential for improving the cell performance. Issues related to doping concentration, surface recombination, and extended region back contact Schottky barrier are investigated.

The modeling work on CdTe structures is based on simulation program, AFORS-HET [27–29]. The software program has been used in the development and design of several solar cells in the past. The device modeling solves relatively large number of nonlinear and tightly coupled partial differential diffusion equations and uses several position-dependent material and transport parameters that make it robust. The device equations are solved over a set of mesh geometry. In addition, for solar cell structures the model includes optical absorption and a broad spectrum of light input that can be

Table 1: Material parameters used in the simulation [10–12].

Parameter	CdTe	CdS	ZnO (TCO)
E_g (eV)	1.42	2.53	3.4
Electron Affinity (eV)	4.28	4.5	4.5
μn (cm^2/v·s)	500	340	100
μp (cm^2/v·s)	60	50	25
Relative Dielectric Constant	10.9	8.9	9
Density of state for electron (cm^{-3})	7.8×10^{17}	2.22×10^{18}	2.22×10^{18}
Density of state for hole (cm^{-3})	1.8×10^{19}	1.8×10^{19}	1.9×10^{19}
Index of Refraction	2.76	2.51	2.006
Doping Density (cm^{-3})	7×10^{16}–7×10^{18} p-type	1×10^{18} n-type	1×10^{18} n-type
ZnO/CdS ΔE_c (eV)		0.0	
ZnO/CdS ΔE_v (eV)		0.87	
CdS/CdTe ΔE_c (eV)	0.22		
CdS/CdTe ΔE_v (eV)	0.89		

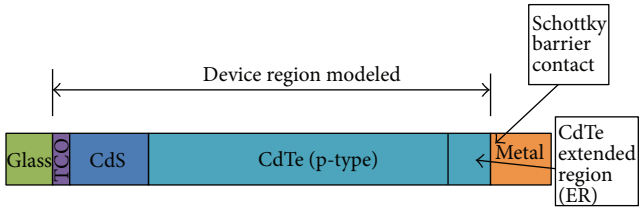

Figure 1: The configuration of a CdTe thin-film solar cell. A 2 μm CdTe layer, a 40 nm CdS layer, and 0.5 μm TCO(ZnO) are assumed for the simulation; layers are not scaled. Light is illuminated from left.

supplied to properly simulate the characteristics of a solar cell. In the next sections we will show in detail that the program works well for CdTe/CdS photovoltaic devices.

2. Device Design and Analysis

The schematic of a CdTe thin-film solar cell used in the simulation with TCO/CdS(n-type)/CdTe(p-type)/metal structure is shown in Figure 1.

In this design, the carrier density of CdTe p-type layer is 7×10^{16} cm^{-3} (similar to the experimental data) with heavy doped CdS n-layer of 1×10^{18} cm^{-3}. The CdTe is a direct bandgap semiconductor with a large absorption coefficient. Because of this important optical property, very thin CdTe layers can be used for photovoltaic applications. For the simulation, we have used a film thickness of 2 μm as in the typical CdTe solar cell manufacturing [30–35]. Table 1 shows the characteristics of ZnO-TCO layer. A 500 nm thick TCO layer with an n-type doping density of 1×10^{18} cm^{-3} is assumed. For this structure, the depletion region is formed in CdTe absorption layer. That is, a 2 μm CdTe cell and a doping density of 7×10^{16} cm^{-3} become fully depleted. It is desirable to have photons absorbed in this region where light induced carriers can be collected with the assistance of the built-in electric field. Similarly, at a wavelength of 600 nm, a 2 μm of CdTe layer will absorb more than 99% of incident light, making CdTe a suitable candidate for absorption material for photovoltaic applications.

Other device parameters are CdS layer with a thickness of a 40 nm and ZnO transparent conductive oxide (TCO) layer with a thickness of 0.5 μm. The TCO layer with a bandgap energy of about 3.4 eV is used to minimize the optical loss where at this high sun energy TCO prevents less blue light from reaching CdTe for a thick CdS layer.

The layer of CdTe is assumed to have an electron affinity of 4.28 eV and a bandgap of 1.42 eV. In order to create an ohmic contact, a metal with a work function greater than or equal to 5.7 eV (the sum of electron affinity and bandgap) is required. As a result most metal contacts applied to p-type CdTe such as copper with work function of 4.6 eV, nickel with 5.1 eV, or titanium with 4.3 eV create nonohmic Schottky type barrier contact which limits the overall performance efficiency of the CdTe cell [36, 37]. As shown in Figure 4, the incorporation of an electron reflector (ER) at back contact is proposed by other investigators to improve the open-circuit voltage of solar cells, and to improve the efficiency of CdTe thin film [3, 8, 10–12].

In a heavily doped p-type metal back contact, the majority of hole carriers are transported by the tunneling in a thin junction of approximately a few nanometer. The optimization and development of the back contact is a limiting factor addressed in this paper and crucial for achieving a high efficiency cell.

3. Experimental Data

A device structure similar to one described in reference [11] is considered. As shown in Figure 3, the measured room temperature dark current-voltage characteristics of the ZnO/CdTe/CdS cell are compared with the simulation result. Data of Table 1 is used in the simulation analysis [10–12]. In addition, a carrier lifetime of 5×10^{-10} s is used. In this model it is assumed that the recombination center is located at the center of the bandgap energy resulting in modeling the recombination of carriers with a constant lifetime. The analysis shows that there is an extended portion of the

Table 2: Current-voltage characteristics of a CdTe cell with different Schottky barrier heights.

Barrier height (eV)	V_{oc} (mV)	J_{sc} (mA/cm^2)	FF (%)	Efficiency (%)
0.1	916	28.36	75.91	19.72
0.2	916	28.35	75.76	19.67
0.4	830	28.23	69.8	16.36

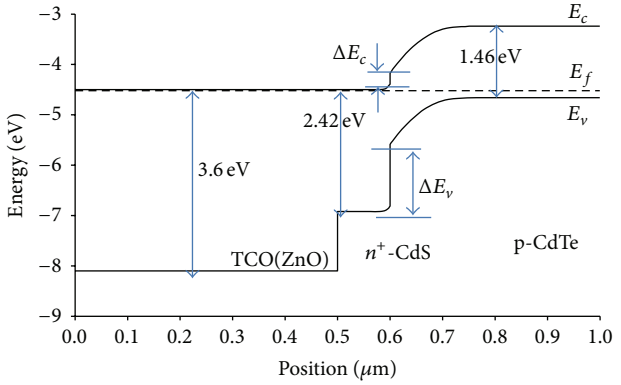

Figure 2: Band diagram of TCO/CdS/CdTe cell without electron reflector layer.

current-voltage curve (less than 0.8 V) that can be modeled with an ideality factor of about 2 where recombination in the space charge region is dominating. In this comparison the goal was not to obtain a best fit but rather to develop a realistic device structure to study the effect of back Schottky contact on the performance of the cell. Here, a structure with the p-type CdTe doping of 7×10^{16} cm^{-3} and a thickness of 2 μm becomes the base device for our optimization. This device shows a maximum short-circuit current density of about 28.4 mA/cm^2 which will be used throughout this study.

Simulation results for a base device show that by reducing the barrier height φe from 0.4 to 0.1 eV a higher open-circuit voltage may be obtained while the short-circuit current remains virtually constant. These results are summarized in Table 2. In addition a higher overall cell efficiency can be achieved with the reduced φe. An optimized device shows a φe of about 0.1 eV. The base device has an efficiency of about 16.38% similar to the experimental data. Moreover, the base device shows an efficiency of about 17.46% assuming an ohmic contact with an infinite surface recombination velocity of 1×10^7 cm/s (Figure 5). We chose the simulation data and analysis mostly around a device with a barrier height of 0.3–0.4 eV as this number is more closely related to a realistic CdTe device structure with back Schottky contact [12, 15–18, 31].

In the absence of an electron reflector or extended region, the band bending of the back surface results in surface recombination degrading the device performance (Figure 2). The surface recombination velocity is a function not only of the material quality and the device but also of the doping level. The exact value of surface recombination velocity is frequently not known but typically extracted from the

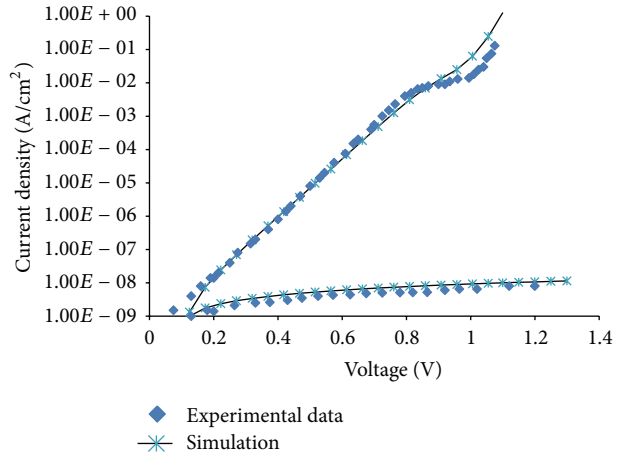

Figure 3: Current-voltage characteristics of thin-film CdS/CdTe cell. The measured experimental data is taken from [11].

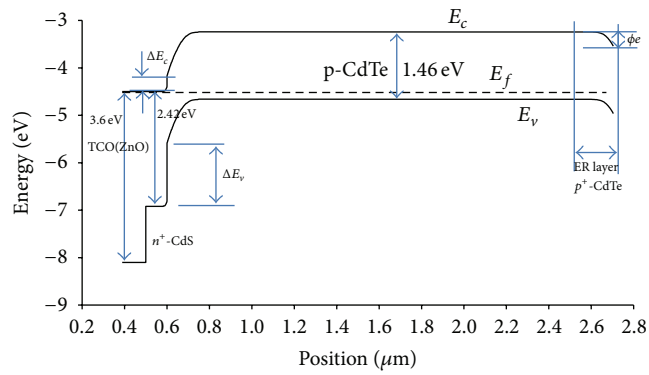

Figure 4: Band diagram of TCO/CdS/CdTe cell with added electron-reflector-extended region (ER layer).

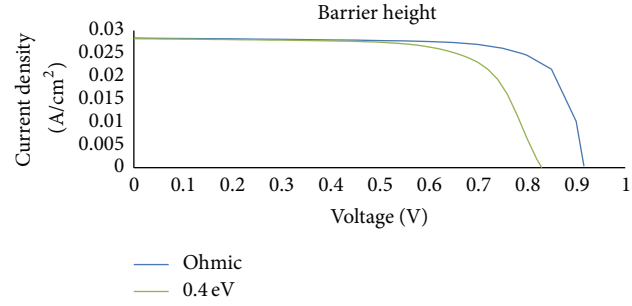

Figure 5: The simulated photocurrent voltage for both ohmic contact and Schottky contact with a barrier height (φe) of 0.4 eV. No extended region is used.

measured data of a given device. The back surface recombination is considered a major limitation factor on a cell's performance in thin devices. The built-in field at the back surface can drive the carriers away from the back surface, thereby affecting recombination rate. In addition, the electric field at back surface may also increase the probability for electron-hole generation near the back contact. A higher

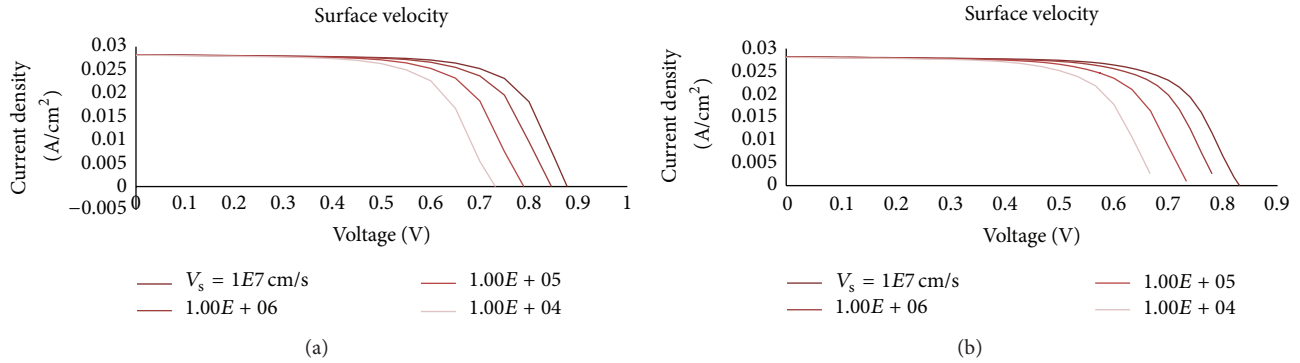

Figure 6: Effect of surface recombination velocity at back contact on cell performance. An ER thickness of 100 nm and a doping density of 7×10^{18} cm^{-3} are assumed; (a) barrier height of 0.1 eV; (b) barrier height of 0.4 eV.

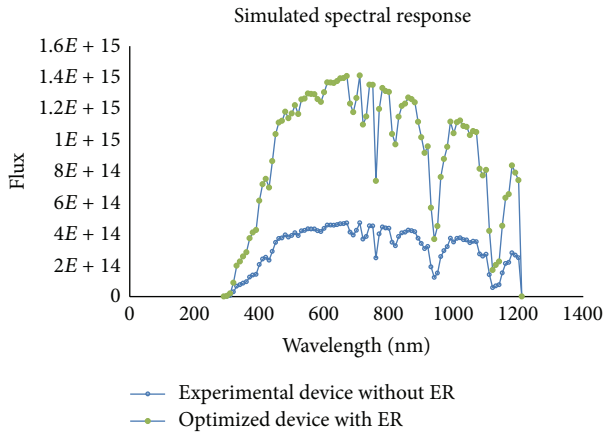

Figure 7: The simulated spectral response of an optimized CdTe cell with 100 nm extended region and a doping of 7×10^{16} cm^{-3}.

velocity is desirable which improves the contact condition toward an ohmic status thus reducing the loss of carriers. As shown in Figure 6, simulation results show that surface recombination at the back contact significantly reduces the open-circuit voltage.

4. Electron Reflector Layer Thickness

For the optimization of the device an offset to the CdTe, absorption layer is considered by adding a CdTe layer as an electron-reflector-extended region (ER), (Figure 4). In addition to CdTe, other materials such as CdZnTe, CdMnTe, and CdMgTe may be employed in creating an ER layer [10, 14, 15, 17, 29, 36].

A thin-layer electron reflector causes the depletion region of the Schottky barrier contact to be narrow where majority of hole carriers can tunnel through minimizing the loss. The simulated spectral density of the CdTe cell with and without the introduction of the ER is shown in Figure 7. As shown in this figure an ER layer may also add an additional absorption layer to the structure thus increasing the spectral response by increasing photogenerated carriers. The thickness of *ER* layer

Table 3: Electron reflector layer thickness and cell performance. A barrier height of 0.3 eV and a doping of 7×10^{16} cm^{-3} are assumed.

ER thickness (nm)	V_{oc} (mV)	J_{sc} (mA/cm^2)	FF (%)	Efficiency (%)
0	869.9	28.27	71.0	17.46
100	872.3	28.3	70.89	17.50
200	875.4	28.31	70.65	17.51
500	883.2	28.33	70.06	17.53

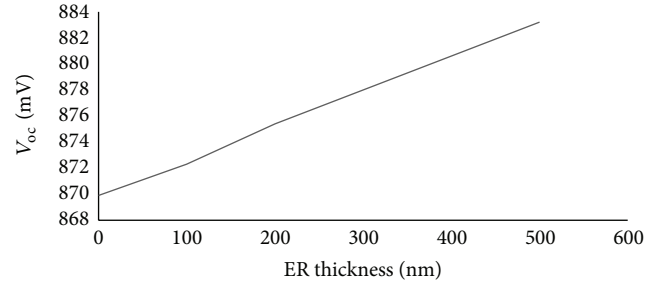

Figure 8: Effect of ER layer thickness on open-circuit voltage of the cell. A doping of 7×10^{16} cm^{-3} is assumed.

Table 4: ER layer with different values of doping density. Thickness of ER layer is 100 nm.

ER with different doping (cm^{-3})	V_{oc} (mV)	J_{sc} (mA/cm^2)	FF (%)	Efficiency (%)
7×10^{16}	872.3	28.3	70.89	17.50
7×10^{17}	877.7	28.29	71.26	17.70
7×10^{18}	891	28.32	71.21	17.97

used in the simulation of spectral response is 100 nm, and the *ER* doping density is assumed to be 7×10^{16} cm^{-3}.

The tradeoff between the open-circuit voltage and short-circuit current when ER is included is shown in the simulated results of Table 3. As shown in Figure 8, the short-circuit current remain relatively constant with the ER layer thickness while the open-circuit voltage increases. In this example the thickness of extended region ranges from 50 nm to 500 nm

Table 5: Cell efficiency with ER layer thickness of 100 nm and doping density of 7×10^{18} cm^{-3}. A barrier height of 0.1 eV is assumed.

ER different thickness (nm)	V_{oc} (mV)	J_{sc} (mA/cm^2)	FF (%)	Efficiency (%)
100	917.6	28.45	75.99	19.83

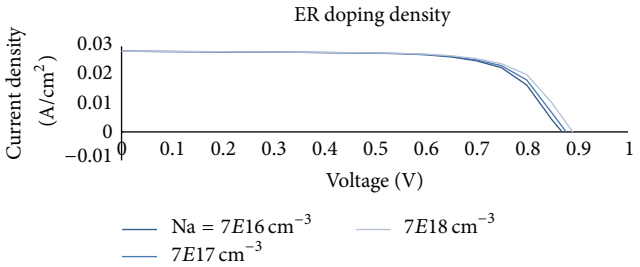

Figure 9: Photocurrent-voltage characteristics of CdTe cell at different doping densities of *ER* layer.

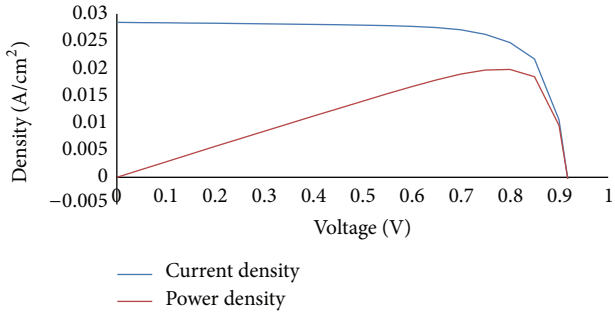

Figure 10: Optimized CdS/CdTe cell with V_{oc} of 917.6 mV, J_{sc} of 28.45 mA/cm^2, and an efficiency of 19.83%.

where the doping density and the barrier height are kept constant at 7×10^{16} cm^{-3} and 0.3 eV, respectively. As indicated earlier in the discussions, the simulation data and analysis are chosen mostly around a device structure with a barrier height of 0.3–0.4 eV as this number is closely related to a realistic CdTe device with Schottky barrier contact [12, 15–18, 31].

Normally the extended layer is heavily doped to minimize the negative effect of the Schottky barrier. Table 4 summarizes the simulated results for an example where the doping density of *ER* layer varied from 7×10^{16} cm^{-3} to 7×10^{18} cm^{-3}. The thickness of *ER* layer and the barrier height are kept constant at 100 nm and 0.3 eV, respectively. Further simulation analysis and results show that the best performance efficiency of about 19.83% may be obtained with an *ER* layer doping of 7×10^{18} cm^{-3} and an *ER* thickness of 100 nm at a barrier height of 0.1 eV.

5. Conclusion

The analysis obtained shows that in the optimization of the cell combining the two mechanisms of heavy doping and extended region are the key parameters to achieve a better cell design. Our results show that in addition to a low surface recombination velocity of 1000 cm/s at back contact and a barrier height of 0.1 eV, an *ER* layer of 100 nm with a doping density of 7×10^{18} cm^{-3} is also required to produce the best cell efficiency performance of 19.83% summarized in Table 5. The photocurrent characteristics of the optimized cell with V_{oc} of 917.6 mV, J_{sc} of 28.45 mA/cm^2, and an efficiency of 19.83% are shown in Figure 10. In the summary a number of different design parameters are used to optimize CdS/CdTe heterojunction thin-film cell (Figure 9). Simulation results show for an optimum efficiency performance a doping density of 7×10^{18} cm^{-3} and ER layer thickness of 100 nm are needed, as summarized in Table 5.

References

[1] G. C. Morris and S. K. Das, "Some fabrication procedures for electrodeposited CdTe solar cells," *International Journal of Solar Energy*, vol. 12, no. 1–4, pp. 95–108, 1992.

[2] S. Ikegami, "CdS/CdTe solar cells by the screen-printing-sintering technique: Fabrication, photovoltaic properties and applications," *Solar Cells*, vol. 23, no. 1-2, pp. 89–105, 1988.

[3] T. L. Chu and S. S. Chu, "High efficiency thin film CdS/CdTe solar cells," *International Journal of Solar Energy*, vol. 12, no. 1–4, pp. 121–132, 1992.

[4] X. Wu, "High-efficiency polycrystalline CdTe thin-film solar cells," *Solar Energy*, vol. 77, no. 6, pp. 803–814, 2004.

[5] V. M. Nikale, S. S. Shinde, C. H. Bhosale, and K. Y. Rajpure, "Physical properties of spray deposited CdTe thin films: PEC performance," *Journal of Semiconductors*, vol. 32, no. 3, Article ID 033001, 2011.

[6] A. Luque and S. Hegedus, *Handbook of Photovoltaic Science and Engineering*, John Wiley & Sons, Chichester, UK, 2003.

[7] V. M. Fthenakis, "Could CdTe PV Modules Pollute the Environment?" Working Paper, National Photovoltaic Environmental Health and Safety Assistance Center, Brookhaven National Laboratory, Upton, NY, USA, 2002.

[8] J. Britt and C. Ferekides, "Thin-film CdS/CdTe solar cell with 15.8% efficiency," *Applied Physics Letters*, vol. 62, no. 22, pp. 2851–2852, 1993.

[9] M. Powalla and D. Bonnet, "Thin-film solar cells based on the polycrystalline compound semiconductors CIS and CdTe," *Advances in OptoElectronics*, vol. 2007, Article ID 97545, 6 pages, 2007.

[10] K. Hsiao, *Electron-reflector strategy for cdte thin-film solar cells [Ph.D. dissertation]*, Colorado State University, 2010.

[11] L. Kosyachenko, "Efficiency of thin-film CdS/CdTe solar cells," in *Solar Energy*, R. D. Rugescu, Ed., pp. 105–130, 2010.

[12] J. Sites and J. Pan, "Strategies to increase CdTe solar-cell voltage," *Thin Solid Films*, vol. 515, no. 15, pp. 6099–6102, 2007.

[13] J. Han, C. Fan, C. Spanheimer et al., "Electrical properties of the CdTe back contact: a new chemically etching process based on nitric acid/acetic acid mixtures," *Applied Surface Science*, vol. 256, no. 20, pp. 5803–5806, 2010.

[14] I. M. Dharmadasa, "Latest developments in CdTe, CuInGaSe2 and GaAs/AlGaAs thin film PV solar cells," *Current Applied Physics*, vol. 9, no. 2, pp. e2–e6, 2009.

[15] S. H. Kim, J. H. Ahn, H. S. Kim, H. M. Lee, and D. H. Kim, "The formation of ZnTe:Cu and CuxTe double layer back contacts for CdTe solar cells," *Current Applied Physics*, vol. 10, no. 3, pp. S484–S487, 2010.

[16] M. A. Matin, M. Mannir Aliyu, A. H. Quadery, and N. Amin, "Prospects of novel front and back contacts for high efficiency cadmium telluride thin film solar cells from numerical analysis," *Solar Energy Materials and Solar Cells*, vol. 94, no. 9, pp. 1496–1500, 2010.

[17] H. Lin, W. Xia, H. N. Wu, and C. W. Tang, "CdS/CdTe solar cells with MoOx as back contact buffers," *Applied Physics Letters*, vol. 97, no. 12, Article ID 123504, 2010.

[18] N. R. Paudel, A. D. Compaan, and Y. Yan, "Sputtered CdS/CdTe solar cells with MoO_{3-x}/Au back contacts," *Solar Energy Materials and Solar Cells*, vol. 113, pp. 26–30, 2013.

[19] T. Surek, "Crystal growth and materials research in photovoltaics: progress and challenges," *Journal of Crystal Growth*, vol. 275, no. 1-2, pp. 292–304, 2005.

[20] H. R. Moutinho, R. G. Dhere, C.-S. Jiang, Y. Yan, D. S. Albin, and M. M. Al-Jassim, "Investigation of potential and electric field profiles in cross sections of CdTe/CdS solar cells using scanning Kelvin probe microscopy," *Journal of Applied Physics*, vol. 108, no. 7, Article ID 074503, 2010.

[21] Y. Ye, L. Dai, T. Sun et al., "High-quality CdTe nanowires: synthesis, characterization, and application in photoresponse devices," *Journal of Applied Physics*, vol. 108, no. 4, Article ID 044301, 2010.

[22] K. W. Böer, "CdS enhances Voc and fill factor in CdS/CdTe and CdS/CuInSe 2 solar cells," *Journal of Applied Physics*, vol. 107, no. 2, Article ID 023701, 2010.

[23] B. Yan, G. Yue, X. Xu, J. Yang, and S. Guha, "High efficiency amorphous and nanocrystalline silicon solar cells," *Physica Status Solidi A*, vol. 207, no. 3, pp. 671–677, 2010.

[24] M. A. Green, "Thin-film solar cells: review of materials, technologies and commercial status," *Journal of Materials Science*, vol. 18, no. 10, supplement 1, pp. S15–S19, 2007.

[25] Z. Fang, X. C. Wang, H. C. Wu, and C. Z. Zhao, "Achievements and challenges of CdS/CdTe solar cells," *International Journal of Photoenergy*, vol. 2011, Article ID 297350, 8 pages, 2011.

[26] N. Romeo, A. Bosio, V. Canevari, and A. Podestà, "Recent progress on CdTe/CdS thin film solar cells," *Solar Energy*, vol. 77, no. 6, pp. 795–801, 2004.

[27] A. Froitzheim, R. Stang, L. Elstner, M. Kriege, and W. Fuhs, *Afors-het: a computer-program for the simulation of heterojunction solar cells to be distributed for public use [M.S. thesis]*, Hahn-Meitner-Institut, Berlin, Germany, 2009.

[28] R. Stangl, J. Haschke, and C. Leendertz, "Numerical simulation of solar cells and solar cell characterization methods: the open-source on demand program AFORS-HET, version 2.4," in *Solar Energy*, 2009.

[29] N. Amin, K. Sopian, and M. Konagai, "Numerical modeling of CdS/CdTe and CdS/CdTe/ZnTe solar cells as a function of CdTe thickness," *Solar Energy Materials and Solar Cells*, vol. 91, no. 13, pp. 1202–1208, 2007.

[30] L. Chen, *Random deposition model of CdS layer in CdSs/CdTe thin-film solar cells [M.S. thesis]*, Colorado State University, 2008.

[31] X. H. Zhao, A. X. Wei, Y. Zhao, and J. Liu, "Structural and optical properties of CdS thin films prepared by chemical bath deposition at different ammonia concentration and S/Cd molar ratios," *Journal of Materials Science*, pp. 1–6, 2012.

[32] T. M. Razykov, N. Amin, B. Ergashev et al., "Effect of CdCl2 treatment on physical properties of CdTe films with different compositions fabricated by chemical molecular beam deposition," *Applied Solar Energy*, vol. 49, p. 35, 2013.

[33] B. A. Korevaar, A. Halverson, J. Cao, J. Choi, C. Collazo-Davila, and W. Huber, "High efficiency CdTe cells using manufacturable window layers and CdTe thickness," *Thin Solid Films*, vol. 535, pp. 229–232, 2013.

[34] B. L. Williams, D. P. Halliday, B. G. Mendis, and K. Durose, "Microstructure and point defects in CdTe nanowires for photovoltaic applications," *Nanotechnology*, vol. 24, no. 13, Article ID 135703, 2013.

[35] T.-C. Hou, Y. Yanga, Z.-H. Lin et al., "Nanogenerator based on zinc blende CdTe micro/nanowires," *Nano Energy*, vol. 2, p. 387, 2013.

[36] A. L. Fahrenbruch and R. H. Bube, *Fundamentals of Solar Cells. PhotoVoltaic Solar Energy Conversion*, Academic Press, New York, NY, USA, 1983.

[37] R. H. Bube, *Photoelectronic Properties of Semiconductors*, Cambridge University Press, Cambridge, UK, 1992.